JACS
JOURNAL OF THE AMERICAN CHEMICAL SOCIETY

ARTICLE

pubs.acs.org/JACS

Energetics and Mechanisms for the Unimolecular Dissociation of Protonated Trioses and Relationship to Proton-Mediated Formaldehyde Polymerization to Carbohydrates in Interstellar Environments

Anton Simakov, Osamu Sekiguchi, Arne Joakim C. Bunkan, and Einar Uggerud*

Mass Spectrometry Laboratory and Centre for Theoretical and Computational Chemistry (CTCC), Department of Chemistry, University of Oslo, P.O. Box 1033 Blindern, N-0315 Oslo, Norway

Supporting Information

ABSTRACT: We report the unimolecular decomposition of protonated glyceraldehyde, $[HOCH_2CH(OH)CHO]H^+$, and protonated dihydroxyacetone, $[HOCH_2C(O)CH_2OH]H^+$. On the basis of mass spectrometric experiments and computational quantum chemistry, we have found that these isomeric ions interconvert freely at energies below that required for their unimolecular decompositions. The losses of formaldehyde and water (the latter also followed by CO loss) are the dominating processes, with formaldehyde loss having the lower energetic threshold. The reverse of the formaldehyde loss, namely, the addition of formaldehyde to protonated glycolaldehyde, appears to be an inefficient reaction at low temperature and pressure in the gas phase, leading to dissociation products. The relevance of these findings to interstellar chemistry and prebiotic chemistry is discussed, and it is concluded that the suggestion made in the literature that successive addition of formaldehyde by proton-assisted reactions should account for interstellar carbohydrates most likely is incorrect.

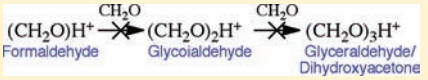

INTRODUCTION

Carbohydrates constitute a fascinating class of organic compounds that act as both energy carriers and key components of information storage molecules in living organisms (ribose and deoxyribose). Formally, monosaccharides are oligomers and polymers of formaldehyde, $(CH_2O)_n$, but the notion that carbohydrates are built up from formaldehyde units is not a theoretical construction, since Butlerov demonstrated long ago in 1861 that formaldehyde oligomerizes into glycolaldehyde, glyceraldehyde, and higher carbohydrates in basic solution (the so-called formose reaction). Langenbeck and co-workers conducted a series of careful kinetic investigations of the formose reaction,[1] and the mechanism, although rather rudimentary, has been attributed to Breslow.[2] The formose reaction plays a similar role in prebiotic chemistry as the oligomerization of HCN into adenine[3,4] and Strecker's classical amino acid synthesis.[5]

The paradigm of prebiotic chemistry is that life evolved from small molecules that in turn formed larger molecules, and that this combined set of molecules eventually assembled into sustainable networks of interconnected chemical reactions.[6] It is furthermore characteristic that living systems are driven by energy gradients and that matter is steadily transported through such systems. In this respect, the formose reaction appears to be central, since it clearly identifies a plausible nonbiological pathway for carbohydrate formation, including the formation of ribose, the sugar part of RNA. This is particularly relevant since it has been proposed that life started out in the form of an RNA world.[7] It is furthermore relevant that formaldehyde[8] and glycolaldehyde[9] (the diose; formally the formaldehyde dimer) are among the more than 150 compounds that to date have been detected in interstellar space.[10] However, attempts to detect the triose members of the family, glyceraldehyde and dihydroxyacetone, in interstellar space have been unsuccessful.[11]

The molecular clouds where most of the known interstellar molecules are found have very low temperatures, which effectively hinders chemical reactions with an energy barrier. Protonation often overcomes this by inducing bond activation of otherwise unreactive molecules, and a manifold of ion−molecule reactions have been invoked to model the chemical complexities of molecular clouds in a consistent and successful manner.[12,13] Approximately 20% of the known interstellar molecules are ionic, of which many are protonated forms, including protonated formaldehyde.[14]

Attempts to identify ion−molecule reactions that lead to a given target (interstellar) molecule may become very tedious and complicated, since they often involve investigating combinations of a large number of ions with a large number of neutrals. An alternative and sometimes more rewarding strategy is to study instead the reverse reaction: the spontaneous unimolecular dissociation of the target molecule. In this way, possible reactant molecules leading to the target may be identified, and details of the energy landscape of the reactions may be revealed. With this approach, it was for example shown that the dissociation of protonated glycine amide $(NH_2CH_2CONH_2)H^+$, a primitive peptide model, gives $NH_3 + CO + CH_2NH_2^+$,[15] all of which are small, stable interstellar molecules.

Received: July 23, 2011
Published: November 09, 2011

In the present context, it is important to mention that Bouchoux and co-workers[16] studied the unimolecular decomposition of protonated glycolaldehyde $[HOCH_2CHO]H^+$ and demonstrated that this molecule exclusively loses water with no trace of formaldehyde loss. This observation strengthens the impression that the first step of the acid-catalyzed formose reaction,

$$CH_2O + CH_2OH^+ \rightarrow [HOCH_2CHO]H^+$$

requires too much energy to be compatible with the conditions of typical molecular clouds. As a matter of fact, the direct reaction between protonated formaldehyde and neutral formaldehyde in the gas phase appears not to lead to dimer formation.[17] However, this does not exclude further CH_2O oligomerization starting from glycolaldehyde, as utilized in the well-known aldol reaction. To test this hypothesis, we studied the fragmentation characteristics of the higher homologues, protonated glyceraldehyde and protonated dihydroxyacetone, and we present the results here. Our study has two aspects: applying mass spectrometry to provide experimental evidence and performing a computational quantum-chemical survey of the appropriate potential energy surfaces.

METHODS

Metastable-Ion and High-Energy Collisional Activation Mass Spectrometry. These measurements were carried out on a double-focusing instrument (Prospec Q, Micromass, Manchester, U.K.) with a three-sector electric/magnetic/electric (EBE) geometry. The compounds were introduced into the electron impact (EI) source via the heatable inlet rod. The electron energy was set at 70 eV, the trap current at 200 μA, the accelerating voltage at 8000 V, and the source temperature at 160−200 °C. Fragmentation of the metastable ions in the third field-free region was registered by selecting the m/z of the precursor ion by the magnetic field and scanning the field of the second electrostatic analyzer [mass-analyzed kinetic energy (MIKE) spectra]. The MIKE spectra are representative for several independent measurements and were averaged from at least 100 consecutive scans. For high-energy collision-induced decomposition (CID), the collision cell was filled with He to a pressure resulting in attenuation of the primary ion beam by 50%, and MIKE−CID spectra were recorded to analyze the fragments.

Low-Energy Variable Collisional Activation Mass Spectrometry. These experiments were performed applying a three-sector mass spectrometer with quadrupole/hexapole/time-of-flight (QHT) geometry (QTOF 2, Micromass/Waters, Manchester, U.K.). The experimental setup consists of an electrospray ionization (ESI) source working at atmospheric pressure. After having entered the high-vacuum region of the apparatus, ions are focused into the quadrupole mass filter. Experiments are done either by setting the quadrupole in broadband mode, effectively letting all ions pass, whereupon a mass spectrum is recorded by means of the time-of-flight (TOF) analyzer, or in narrow-band mode, in which the quadrupole voltages are set to transmit only ions with the m/z value of interest. This is done at a sufficiently high mass resolution to avoid passage of ions with $m/z \pm 1$. The ions selected in this way are then decelerated or accelerated to a variable energy in the range E_{lab} = 0.2−20 eV before entering a collision cell (path length 16 cm). The latter includes a hexapole ion guide. In this region, the selected ions are collided with argon at a low pressure. To reduce the occurrence of multiple collisions for any given ion, attenuation of the parent ion beam was kept below 10% when obtaining energy-resolved mass spectra. After leaving the collision cell, the ions are accelerated to a few electron volts and then transferred into the TOF region, which is kept at high vacuum (2×10^{-7} mbar). The TOF analyzer is of the reflectron type, and the ion beam is extracted and accelerated to 9.1 keV in a direction orthogonal to the ion optical axis of the QH assembly by applying a high-voltage pulse to a set of acceleration electrodes. The duty cycle of the TOF analyzer is fixed to allow all ions in a wide mass range to arrive before sending off the next burst of ions, and the ion count rate is adjusted to allow for a sufficiently wide linear dynamic range. The mass resolution of the TOF analyzer was set to $m/\Delta m$ = 5000 (fwhm). Typically, for each reaction studied, time-of-flight spectra are accumulated for 3 min for each chosen value of E_{lab}.

Ion−Molecule Reactions and FT-ICR Mass Spectrometry. Protonated glycolaldehyde was produced in an external ion source using chemical ionization with methane. The ions formed in the source were transferred to the cell of a Fourier transform ion cyclotron resonance (FT-ICR) mass spectrometer (Bruker 4.7 T Bio Apex, Billerica, MA). The neutral substrate formaldehyde was dispensed into the FT-ICR cell through a leak valve ($p = 2.0 \times 10^{-9}$ to 1.5×10^{-8} mbar) upon vaporization of a paraformaldehyde sample (98%, Sigma-Aldrich). Ion isolation and all subsequent isolation steps were performed using a computer-controlled ion ejection protocol combining single-frequency ion ejection pulses with frequency sweeps. Briefly, all ions except the chosen reactant ion were ejected from the cell by this procedure. After this process, the ions were allowed to react freely with the substrate for a time delay of 1−30 s before a mass spectrum was recorded.

Quantum-Chemical Calculations. Quantum-chemical calculations were done using the Gaussian 09 program system.[18] Complete optimization of the molecular geometries was done using the B3LYP hybrid density functional with the 6-31G(d) basis set [B3LYP/6-31G(d)] and second-order Møller−Plesset perturbation theory with same basis set [MP2/6-31G(d)]. All stationary points were subject to complete geometry optimization, including a check for the correct number of negative Hessian eigenvalues and imaginary vibrational frequencies. Great care was taken to localize the global minima for the neutral and protonated forms of glyceraldehyde and dihydroxyacetone. Transition states (TSs) were carefully checked to ensure that they connect the actual minimum-energy structures. Intrinsic reaction coordinate (IRC) calculations were performed for all TSs. The IRC routine failed numerically in a number of the cases reported here. In these ill cases, we were careful to verify the connections not only on the basis of the vibrational motion of the reaction coordinate at the TS but also by showing that extrapolation in the forward and backward directions, respectively, led to geometries that upon minimization gave the indicated minima. To obtain more accurate estimates for the energies, G4 theory calculations were done. G4 is a composite technique that involves geometry optimizations and frequency calculations at rather moderate levels of theory but with a scheme for extrapolating the energy to include essentially both the qualities of a large atomic basis set and dynamic electron correlation to the CCSD(T) level.[19] G4 employs B3LYP/6-31G(2df,p) for geometry optimization and frequency calculations. The MP2 and B3LYP geometries and relative energies were found to be in good agreement. For the reactions and molecules studied here, this consistency and comparison with known accurate thermochemical data provide support for the claimed accuracy of the G4 method (i.e., within $\pm$10 kJ mol^{-1}).

RESULTS AND DISCUSSION

Electron Impact Ionization. The EI mass spectra obtained for glyceraldehyde contain peaks above the monomer mass at m/z 91, 101, and 121, and that of dihydroxyacetone has peaks at m/z 91 and 149. The spectrum for glyceraldehyde is similar to that reported by Brittain et al.[20] These authors provided experimental evidence in favor of the covalently bonded dimer, 2,5-dihydroxymethyl-2,5-dihydroxy-1,4-dioxane, being present in the gas phase but showing that the radical cation is unstable toward dissociation, and they suggested a probable mass spectral dissociation mechanism. In this context, we also note that the two

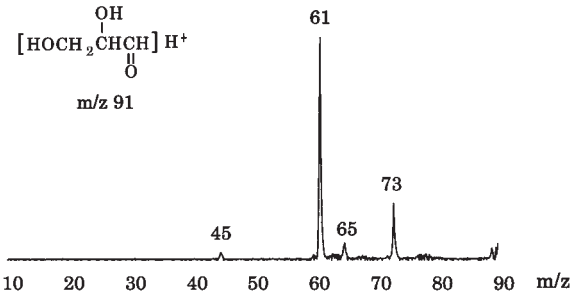

Figure 1. MIKE spectrum of m/z 91 from EI-ionized glyceraldehyde. The peak at m/z 65 is absent from the corresponding CH_4 CI spectrum.

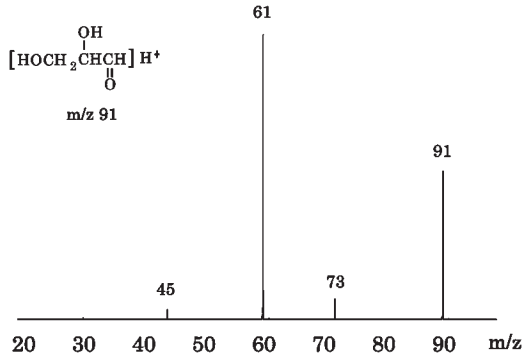

Figure 2. Low-energy (E_{lab} = 10 eV, nominally $p > 5 \times 10^{-3}$ mbar Ar) CID mass spectrum of m/z 91 from ESI-ionized glyceraldehyde.

mass spectra are clearly different from that of the isomeric glucose. The MIKE and MIKE−CID spectra of the ions with m/z 91 ($C_3H_7O_3^+$) were recorded (Figure 1). The MIKE spectra are identical for the two compounds, with dominant peaks at m/z 73 (loss of H_2O) and m/z 61 (loss of CH_2O) and smaller peaks at m/z 45 and m/z 65. The peak at m/z 65 is probably from an unidentified isobaric overlap (also see below). The separately recorded MIKE spectrum of the ion with m/z 61 exhibits essentially one peak at m/z 43 due to H_2O loss. The MIKE−CID spectra are similar but have slightly different intensities for some of the less abundant peaks.

In the methane CI mass spectra of these compounds, more intense signals for m/z 91 were observed. It is, however, significant that the MIKE and MIKE−CID spectra for m/z 91 under CI were nearly identical to those obtained under EI conditions, except that there was no signal for m/z 65 with CI. Furthermore, the MIKE and MIKE−CID spectra for m/z 91 obtained using hydrogen as CI gas were essentially identical to those using methane, suggesting that the ion beams do not contain higher-energy isomers.

Electrospray Ionization. Protonated dihydroxyacetone and protonated glyceraldehyde ($C_3H_7O_3^+$, m/z 91) were formed by ESI of the respective neutrals. Mass-selected m/z 91 was subjected to CID, and the spectrum for protonated glyceraldehyde is reproduced in Figure 2. Significant fragments were found at m/z 73, 61, and 45, with a weak fragment at m/z 31. No signal was found at m/z 65, strengthening the hypothesis given above that this is due to a contaminant exclusive to EI. It is noteworthy that the soft ESI method upon low-energy (eV) collisional activation gives essentially the same MIKE spectra obtained using EI and CI. This provides a strong indication that the same

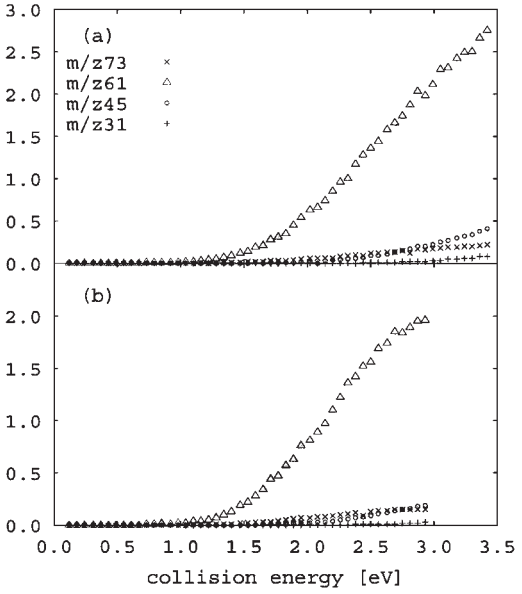

Figure 3. Energy-resolved fragment ion abundances (in % of total) of (a) protonated glyceraldehyde and (b) protonated dihydroxyacetone at nominally $p = 5 \times 10^{-5}$ mbar Ar. Collision energy is in the center-of-mass frame.

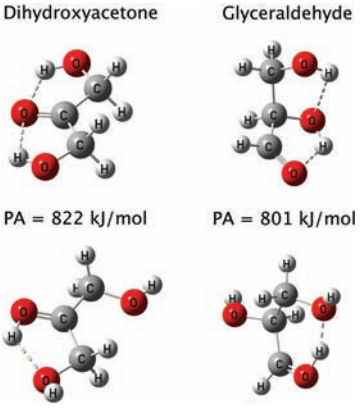

Figure 4. Ball-and-stick models of the most stable forms of dihydroxyacetone (**d1**) and glyceraldehyde (**g1**) (upper row) and their respective protonated forms **pd1** and **pg1** (lower row).

ion structures are involved in the unimolecular dissociation in all cases, involving similar portions of the (ground-state) potential energy surface, and that unknown high-energy isomers are unlikely to be involved.

The relative CID fragment ion abundances as function of energy are reproduced in Figure 3. The curves indicate a lower threshold and steeper onset for ions with m/z 61 than the other fragment ions.

Sites of Protonation and Proton Affinities. Both 1,3-dihydroxyacetone and D-glyceraldehyde may exist in several conformers, and the relative conformer stability is to a large degree dictated by intramolecular hydrogen bonding. This is reflected in our G4 calculations that reproduce the literature, with **d1**[21,22] and **g1**[22,23] being the most stable forms, respectively (Figure 4). Protonation of **d1** and **g1** provides even higher structural complexity, since any of the oxygen atoms may be protonated.

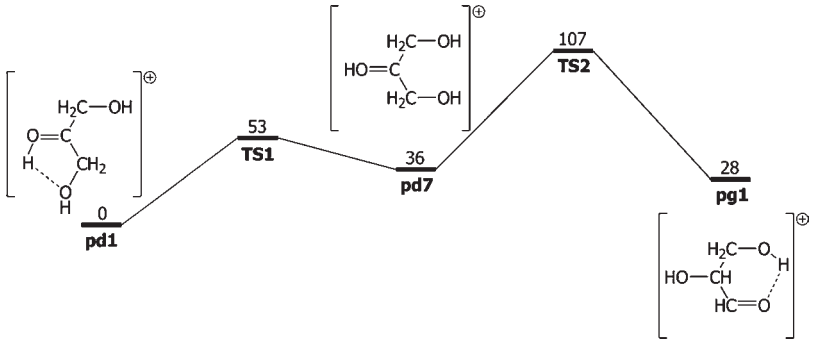

Figure 5. Potential energy diagram for the isomerization between the most stable protonated forms of dihydroxyacetone and glyceraldehyde (energies in kJ/mol).

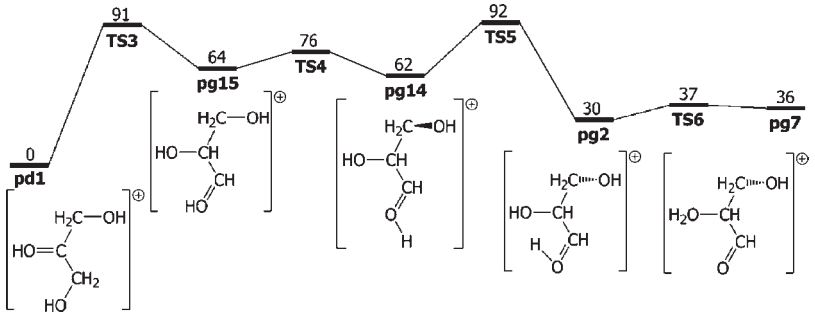

Figure 6. Potential energy diagram illustrating the first common pathway for isomerization prior to formaldehyde loss and water + carbon monoxide loss (energies in kJ/mol).

The most stable forms, taking all isomeric and conformeric possibilities into consideration, are **pd1** and **pg1**, respectively (Figure 4). Of these two, protonated dihydroxyacetone (**pd1**) was calculated to be 28 kJ mol^{-1} lower in energy than protonated glyceraldehyde (**pg1**). For this reason, we set **pd1** to be our zero point of reference. On the basis of the estimated relative enthalpies of formation at 298 K, we obtain the proton affinities PA(**d1**) = 822 kJ mol^{-1} and PA(**g1**) = 801 kJ mol^{-1}. The values of these quantities are not essentially affected by replacing the B3LYP/6-31G(d,p) geometries with the very similar B3LYP/6-311+(d,p) geometries. We are not aware of any experimental proton affinity values for these compounds. On the basis of the larger polarizabilities and more options for intramolecular hydrogen bonds, it is not unexpected that the values are higher than the established proton affinities of the smaller but related molecules formaldehyde,[24] methanol,[24] and glycolaldehyde[16] (713, 754, and 783 kJ mol^{-1}, respectively). For both protonated dihydroxyacetone and protonated glyceraldehyde, the most stable form corresponds to geometries where the proton is bridged between the carbonyl and hydroxyl oxygens but located closer to the carbonyl oxygen. For each there exists a manifold of forms within the energy window 0−100 kJ mol^{-1}. We will not go into the details of this, but we note that C−C bond rotation and proton transfer between the different oxygens may occur swiftly within this energy window.

Isomerization. On the background of the well-known reversible ketose−aldose isomerization reaction, which may take place under acidic conditions in solution,[25] we were interested to see whether gaseous **pd1** and **pg1** interconvert at energies compatible with the experimental conditions described above. The mechanism is depicted in Figure 5. Starting with protonated dihydroxyacetone in its most stable form, **pd1**, the first step corresponds to a low-energy C−C bond rotation involving **pd7** as an intermediate. From this intermediate, a simple hydride transfer from a terminal to the central carbon completes the reaction, directly giving the most stable form of protonated glyceraldehyde, **pg1**. In the key transition structure **TS2**, the hydrogen is approximately midway, bridging the two carbon atoms. Similar hydride transfer mechanisms have been described on the basis of quantum-chemical calculations of small model systems by Zheng et al.[26] The computed G4 energies provide a critical energy in the forward direction of 107 kJ mol^{-1}, which is higher than the energy required for a proton to move freely between the oxygens of each of the two protonated molecules but clearly lower than required for fragmentation to occur (see below). In terms of energy requirements, this means that irrespective which of the two neutral compounds that is used as the original precursor, any unimolecular dissociation will occur from a common **pd1**/**pg1** pool rather from separated **pd1** or **pg1**.

Loss of Formaldehyde. From the experimental observations reported above, it is clear that loss of formaldehyde is the dominating dissociation reaction. In our computational study, this reaction was found to occur in six distinct steps. The corresponding potential energy diagram connecting the reactant and products are depicted in Figures 6 and 7. Starting from the most stable form of protonated hydroxyacetone, **pd1**, the first step is a rather energy-demanding hydride shift to **pg15**. This is followed by a C−O rotation to give **pg14** and then a C−C rotation to **pg2** (Figure 6). From **pg2**, heterolytic C−C bond dissociation leads to the complex between *cis*-1,2-dihydroxyethene and protonated formaldehyde, **INT1** (Figure 7). We note that this is the reverse of an acid-catalyzed aldol addition.

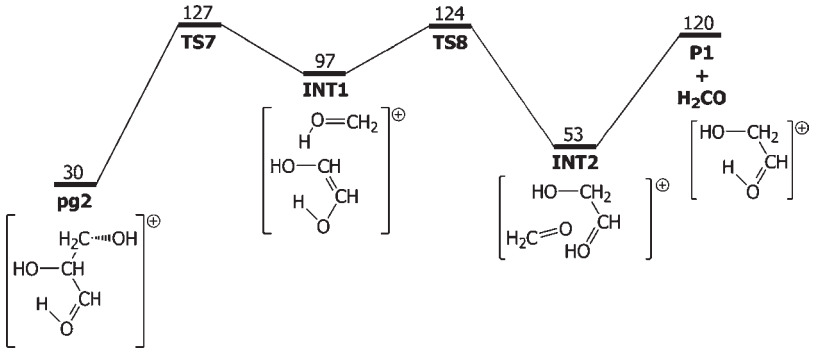

Figure 7. Potential energy diagram illustrating formaldehyde loss from protonated glyceraldehyde (energies in kJ/mol).

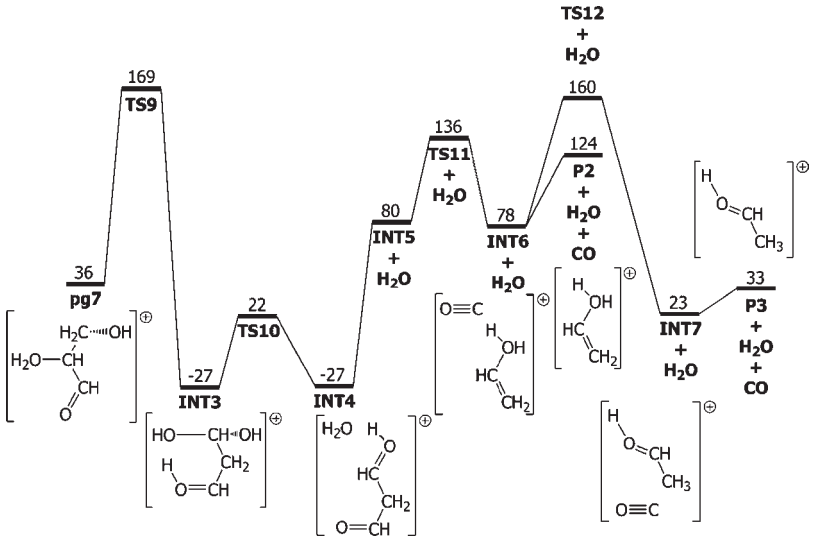

Figure 8. Potential energy diagram illustrating water loss from protonated glyceraldehyde, including the subsequent loss of carbon monoxide (energies in kJ/mol).

Intracomplex proton transfer then gives a complex between formaldehyde and protonated glycolaldehyde, **INT2**, which finally dissociates to give the products, protonated glycolaldehyde (**P1**) plus formaldehyde. The rate-determining step of the complete retro-aldol sequence is passage of **TS7** at 127 kJ mol^{-1}, which we note is higher in energy than the products at 120 kJ mol^{-1}. In essence, the energy diagrams in Figure 5 − 7 provide a consistent reaction mechanism for formaldehyde loss occurring from both protonated dihydroxyacetone and protonated glyceraldehyde.

Loss of Water and Subsequently Carbon Monoxide. Like formaldehyde loss, our calculations indicate that water loss also occurs via the protonated glyceraldehyde basin of the potential energy surface, more precisely via the intermediate $HOCH_2CH(OH)CHOH^+$ (**pg2**), which is formed as explained above (Figure 6). From this intermediate, proton transfer from the carbonyl group to the central hydroxyl group gives $HOCH_2CH(OH_2^+)CHO$ (**pg7**). Continuing now to Figure 8, one sees that from this structure an embryonic water molecule is loosened from the carbon skeleton by stretching of the central C−O bond. In parallel with this movement, a hydride is transferred in a "hidden" manner from the terminal methylene to the gradually evolving carbocationic center at the central carbon atom. This eventually leads to the complex between protonated malonaldehyde and water (**INT4**). However, in strict topographic terms, the transition structure **TS9** connects the minima corresponding to **pg7** and the intermediate **INT3** (protonated hydrated malonaldehyde), in which the water in the latter has been transferred to the terminal carbon atom while the proton ends up at the more basic carbonyl oxygen. The thermochemically favorable **INT4** and **INT3** are connected by the low-lying **TS10**. Finally, water is completely liberated, leaving behind protonated malonaldehyde (**INT5**, m/z 73) as the ionic product. The subsequent loss of carbon monoxide occurs from **INT5** via **TS11** and the product complex **INT6**, which finally produces protonated hydroxyethene (**P2**, m/z 45) as the ionic product. An alternative pathway for CO loss exists, namely, the one leading to protonated acetaldehyde (**P3**). However, the barrier for the intramolecular proton transfer requires passage of **TS12** at the rather unfavorable energy of 160 kJ mol^{-1}. The calculated highest-energy barrier, due to **TS9**, is at 169 kJ mol^{-1}, which is clearly higher than the barrier calculated for the loss of formaldehyde, in good agreement with the experimental observations. We have looked for alternative routes for production of ions with m/z 45, in particular routes for the direct loss of formic acid, HCOOH, instead of H_2O + CO formed in a stepwise mechanism, but these efforts gave only very high energy structures of doubtful chemical relevance.

dx.doi.org/10.1021/ja206600w |*J. Am. Chem. Soc.* 2011, 133, 20816–20822

Probing the Reverse Reaction: Formaldehyde Addition. From Figures 6 and 7, it is clear that addition of formaldehyde to protonated glycolaldehyde is exothermic by 90 kJ mol^{-1} to produce protonated glyceraldehyde and 120 kJ mol^{-1} to produce protonated dihydroxyacetone. On the other hand, according to the potential energy diagram in Figure 7, the reverse reaction of adding formaldehyde to protonated glycolaldehyde has a barrier of 7 kJ mol^{-1} (**TS7**). This value should of course not be taken too literally. Taking the estimated accuracy of the G4 method into account, the possibility exists that the actual barrier is higher, lower, or even absent. In the latter case, an efficient mechanism for C−C bond formation could exist, with important consequences for interstellar carbohydrate chemistry, as outlined in the Introduction. To test this hypothesis, we monitored the products of the ion−molecule reaction between protonated glycolaldehyde and formaldehyde using an FT-ICR mass spectrometer. We observed only a slow reaction: after a reaction time of 30 s at $p = 1.0 \times 10^{-8}$ mbar, corresponding to a bimolecular rate coefficient of the order of 10^{-11} cm^3 s^{-1}, the relative ion abundances amounted to m/z 31 (39%), m/z 73 (29%), m/z 61 (27%), m/z 43 (2%), and minor peaks (3%), which are those expected on the basis the intermediacy of a short-lived protonated glyceraldehyde molecule that decomposes unimolecularly. The peak at m/z 31 is probably due to direct endothermic proton transfer. Both these observations are indicative of superthermal ion velocities, an inevitable result of the ion trapping. The key observation of relevance to interstellar chemistry is, however, that we observed no signs of stable adducts with m/z 91 corresponding to ion−molecule complexes or protonated trioses. We here take into account the fact that short-lived adducts may be formed but in the absence of cooling (radiatively or by third-body collisions) will back-dissociate into the reactants. These considerations have to be borne in mind when extrapolating the FT-ICR results to interstellar chemistry (see the paragraph on the kinetic calculations below).

In interstellar space, protonation of glycolaldehyde may lead to more highly excited species than those considered here. Typically, protonation of glycolaldehyde by the abundant species H_3^+ is exothermic by 360 kJ mol^{-1}. If we (somewhat arbitrarily) assume that 50% of this extra energy ends up as excitation of protonated glycolaldehyde,[27,28] the energy content amounts to 180 kJ mol^{-1}. Bouchoux et al.[16] investigated protonated glycoladehyde, its isomers, and unimolecular dissociation. They identified two low-energy isomers corresponding to protonation at the carbonyl and hydroxyl oxygens. Interestingly, they did not consider a third isomer, formally corresponding to oxygen-protonated dihydroxyethene, which has the potential to react with formaldehyde via intermediates **INT1** and **INT2** in Figure 7. According to quantum-chemical calculations (not shown here), this species corresponds to a potential energy minium that is 100 kJ mol^{-1} higher in energy than the most stable form of protonated glycolaldehyde. On the other hand, rearrangement of protonated glycolaldehyde into this isomeric form would require the passage of a TS at 214 kJ mol^{-1}. It therefore seems rather unlikely that protonation, even by H_3^+, would allow for transfer of enough energy to *irreversibly* produce the potentially more reactive $HOCH{=}CHOH_2^+$.

For an ion−molecule reaction to be of significance to interstellar chemistry, it is necessary for the reaction rate to be comparable with the reactant collision frequency.[12] The physical conditions in the FT-ICR cell are substantially different from those usually encountered in molecular clouds, in particular regarding the pressure, a fact that may have considerable impact on the reaction rates. We therefore decided to model the kinetics. On the basis of our potential energy surface model, we calculated reaction rates for all steps along the following sequence:

$$\mathbf{P1} + CH_2O \underset{k_{-1}}{\overset{k_1}{\rightleftarrows}} \mathbf{INT2} \underset{k_{-2}}{\overset{k_2}{\rightleftarrows}} \mathbf{INT1} \underset{k_{-3}}{\overset{k_3}{\rightleftarrows}} \mathbf{pg2}$$

Rate coefficients as functions of energy for the unimolecular steps were obtained using Rice−Ramsperger−Kassel−Marcus (RRKM) theory with vibrational frequencies and relative energies from the G4 calculations. For the bimolecular association reaction (k_1), we applied the inverse Laplace transform of a weakly temperature-dependent semi-Arrhenius type $k(T)$ expression, with values being close to 1×10^{-9} cm^3 s^{-1} at room temperature. Details are given in the Supporting Information. In vacuum (no termolecular stabilization) below 127 kJ mol^{-1} (corresponding to the low temperatures of interstellar molecular clouds), the barrier at **TS7** efficiently prevents any reactions from occurring. A few kJ mol^{-1} above this, the rate coefficient for back-dissociation into reactants (k_{-1}), which is affected by a considerable translational partition function contribution, is several order of magnitudes larger than k_2, the rate coefficient for passage of the first energy barrier, **TS8**. This prevents any efficient reaction even for reactants at room temperature (**P1** + CH_2O are at 120 kJ mol^{-1} on our energy scale; Figure 7). This is in good agreement with Brauman's empirical rule-of-thumb, which states that a room-temperature ion−molecule reaction with an efficient chemical barrier of +5 kJ mol^{-1} is slowed by a factor of 1000 relative to the collision frequency.[29] In comparison with a typical interstellar molecular cloud, the pressure inside the FT-ICR cell is perhaps 12−13 orders of magnitude higher, amounting in our experiments to 10^{-8} mbar. Nevertheless, this approximately corresponds to a collision frequency of only 1 Hz, which at room temperature is far too small to enhance the reactivity through trapping of intermediates (**INT2** and **INT1**) by stabilizing third-body collisions to any appreciable extent. Our simulations show less than 2 % adduct/product concentration after an integration time of 10 s. In this respect, the FT-ICR results are indicative of the reactivity also at lower pressures and temperatures, as in interstellar space. We will again emphasize that these arguments are critically dependent on the actual barrier heights and also mention that any radiative processes have been neglected in our treatment.

One noticeable example of an exothermic reaction of putative astrophysical relevance that does not occur because of a chemical barrier is $H_2CO^+ + H_2$, which does not form CH_3OH^+.[30] In addition, we need to mention that $NH_4^+ + C_2H_4$ gives a hydrogen-bonded adduct at low temperatures[31] rather than forming the covalently bonded $C_2H_5NH_3^+$, which would be exothermic by 109 kJ mol^{-1}, while $H_3O^+ + C_2H_2$ gives a mixture both of the stable covalent CH_3CHOH^+ adduct and a higher-energy hydrogen-bonded adduct.[32]

■ CONCLUSION

As reported above, the computed potential energy diagrams appear to be consistent with our experiments. The higher abundance and the lower energetic threshold observed for the loss of formaldehyde match the model potential energy data that suggest a 42 kJ mol^{-1} lower energy demand for this process relative to water loss (**TS7** vs **TS9**). Moreover, except for a constant factor, the curves for loss of H_2O (giving m/z 73) and

loss of H_2O + CO (giving m/z 45) are superimposable, which is easy to understand since they have a common rate-determining step (**TS9**).

The suggestion that addition of formaldehyde to protonated glycolaldehyde is a slow reaction, as probed in the FT-ICR experiment and substantiated by the kinetic analysis, suggests that there is a barrier (estimated to be +7 kJ mol^{-1} from the quantum-chemical calculations) and indicates that this pathway for interstellar production of the protonated trioses is unlikely to occur with any measurable rate in the isolated gas phase at low temperature and pressure. In the case that proton-assisted oligomerization of formaldehyde is of any relevance to interstellar chemistry, it must be by other means. These observations, taken together with the previously published report by Bouchoux et al.[16] showing that protonated glycolaldehyde loses water only in unimolecular dissociation, point to the conclusion that successive addition of formaldehyde molecules, assisted by protonation (acid-catalyzed formose reaction/aldol addition), is at best an extremely inefficient process for carbohydrate formation in molecular clouds.

■ ASSOCIATED CONTENT

Supporting Information. Optimized molecular geometries and energies and complete ref 18. This material is available free of charge via the Internet at http://pubs.acs.org.

■ AUTHOR INFORMATION

Corresponding Author
einar.uggerud@kjemi.uio.no

■ ACKNOWLEDGMENT

This work was supported by the Norwegian Research Council by Grant 179568/V30 to the Centre of Theoretical and Computational Chemistry through their Centre of Excellence Program, NOTUR, for generous computational resources. We are also grateful to the reviewers for excellent suggestions.

■ REFERENCES

(1) Langenbeck, W. *Tetrahedron* **1958**, *3*, 185.
(2) Breslow, R. *Tetrahedron Lett.* **1959**, *1*, 22.
(3) Oró, J. *Biochem. Biophys. Res. Commun.* **1960**, *2*, 407.
(4) Ferris, J. P.; Edelson, E. H.; Mount, N. M.; Sullivan, A. E. *J. Mol. Evol.* **1979**, *13*, 317.
(5) Strecker, A. *Annalen* **1854**, *91*, 349.
(6) Orgel, L. E. *Proc. Natl. Acad. Sci. U.S.A.* **2000**, *97*, 12503.
(7) Woese, C. W. *The Genetic Code: the Molecular Basis for Gene Expression*; Harper and Row: New York, 1968.
(8) Snyder, L. E.; Buhl, D.; Zuckerman, B.; Palmer, P. *Phys. Rev. Lett.* **1969**, *22*, 679.
(9) Hollis, J. M.; Lovas, F. J.; Jewell, P. R. *Astrophys. J. Lett.* **2000**, *540*, L107.
(10) Müller, H. S. P.; Schlöder, F.; Stutzki, J.; Winnewisser, G. *J. Mol. Struct.* **2005**, *742*, 215; http://www.astro.uni-koeln.de/cdms/ (accessed July 23, 2011).
(11) Hollis, J. M.; Jewell, P. R.; Lovas, F. J.; Remijan, A.; Møllendal, H. *Astrophys. J. Lett.* **2004**, *610*, L21.
(12) Herbst, E. *Chem. Soc. Rev.* **2001**, *30*, 168.
(13) Dyson, J. E.; Williams, D. A. *The Physics of the Interstellar Medium*; Institute of Physics Publishing: Philadelphia, 1997.
(14) Ohishi, M.; Ishikawa, S.-i.; Amano, T.; Oka, H.; Irvine, W. M.; Dickens, J. E.; Ziurys, L. M.; Apponi, A. J. *Astrophys. J. Lett.* **1996**, *471*, L61.
(15) Lin, H.-Y.; Ridge, D. P.; Uggerud, E.; Vulpius, T. *J. Am. Chem. Soc.* **1994**, *116*, 2996.
(16) Bouchoux, G.; Penaud-Berruyer, F.; Bertrand, W. *Eur. J. Mass Spectrom.* **2001**, *7*, 351.
(17) Jalbout, A. F.; Abrell, L.; Adamowicz, L.; Polt, R.; Apponi, A. J.; Ziurys, L. M. *Astrobiology* **2007**, *7*, 433.
(18) Frisch, M. J.; et al. *Gaussian 09*; Gaussian, Inc.: Wallingford, CT, 2009.
(19) Curtiss, L. A.; Redfern, P. C.; Raghavachari, K. *J. Chem. Phys.* **2007**, *126*, No. 084108.
(20) Brittain, E. F. H.; George, W. O.; Collins, G. C. S. *J. Chem. Soc. B* **1971**, 2414.
(21) Dorofeeva, O. V.; Vogt, N.; Vogt, J.; Popik, M. V.; Rykov, A. N.; Vilkov, L. V. *J. Phys. Chem. A* **2007**, *111*, 6434.
(22) Lovas, F. J.; Suenram, R. D.; Plusquellic, D. F.; Møllendal, H. *J. Mol. Spectrosc.* **2003**, *222*, 263.
(23) Vogt, N.; Atavin, E. G.; Rykov, A. N.; Popov, E. V.; Vilkov, L. V. *J. Mol. Struct.* **2009**, *936*, 125.
(24) Lias, S. G.; Rosenstock, H. M.; Deard, K.; Steiner, B. W.; Herron, J. T.; Holmes, J. H.; Levin, R. D.; Liebman, J. F.; Kafafi, S. A.; Bartmess, J. E.; Hunter, E. F.; Linstrom, P. J.; Mallard, W. G. In *NIST Chemistry Webbook*, 2011; http://webbook.nist.gov/chemistry (accessed July 23, 2011).
(25) Harris, D. W.; Feather, M. S. *J. Am. Chem. Soc.* **1975**, *97*, 178.
(26) Zheng, Y.-J.; Merz, K. M.; Farber, G. K. *Protein Eng.* **1993**, *6*, 479.
(27) Bueker, H.-H.; Helgaker, T.; Ruud, K.; Uggerud, E. *J. Phys. Chem.* **1996**, *100*, 15388.
(28) Li, Y.; Farrar, J. *J. Chem. Phys.* **2004**, *120*, 199.
(29) Brauman, J. I. *J. Mass Spectrom.* **1995**, *30*, 1649.
(30) Francis, G. J.; Wilson, P. F.; Maclagan, R. G. A. R.; Freeman, C. G.; Meot-Ner, M.; McEwan, M. J. *J. Phys. Chem. A* **2004**, *108*, 7548.
(31) Meot-Ner, M.; Deakyne, C. A. *J. Am. Chem. Soc.* **1985**, *107*, 474.
(32) Fairley, D. A.; Scott, G. B. I.; Freeman, C. G.; Maclagan, R. G. A. R.; McEwan, M. J. *J. Chem. Soc., Faraday Trans.* **1996**, *92*, 1305.